

MOLPHARM/2019/118190.R2

LUF7244 plus dofetilide rescues aberrant K_v11.1 trafficking and produces functional I_{Kv11.1}

M. Qile¹, Y. Ji¹, T.D. Golden², M.J.C. Houtman¹, F. Romunde¹, D. Fransen¹,
W.B. van Ham^{1,3}, A.P. IJzerman⁴, C.T. January⁵, L.H. Heitman⁴, A. Stary-
Weinzinger³, B.P. Delisle², M.A.G. van der Heyden^{1*}

¹Department of Medical Physiology, University Medical Center Utrecht,
3584CM Utrecht, The Netherlands; ²Department of Physiology, University of
Kentucky, Lexington, 40536 Kentucky, USA; ³Department of Pharmacology
and Toxicology, University of Vienna, 1090 Vienna, Austria; ⁴ Leiden Academic
Centre for Drug Research, Division of Drug Discovery and Safety, 2333CC
Leiden, The Netherlands; ⁵Department of Medicine, University of Wisconsin,
Madison, 53792 Wisconsin, USA.

M. Qile and Y. Ji contributed equally

21 Running title: Dofetilide+LUF7244 rescues K_v11.1 trafficking and restores

22 I_{Kv11.1}

23

24 * Corresponding author

25 Dr. M.A.G. van der Heyden

26 Dept of Medical Physiology, DH&L, Yalelaan 50

27 3584 CM Utrecht, The Netherlands.

28 Phone: +31 88 7558901

29 Email: m.a.g.vanderheyden@umcutrecht.nl

30

31 Text pages: 44

32 Tables: 0

33 Figures: 6

34 References: 48

35 Abstract: 250

36 Introduction: 742

37 Discussion: 1057

38

39 Abbreviations:

40 APD: action potential duration; cAVB: chronic atrio-ventricular block; hiPSC,

41 human-induced Pluripotent Stem Cell; MD: molecular dynamics; NRVM:

42 neonatal rat ventricular myocytes; SR: sinus rhythm; WT: wild type.

Abstract

K_v11.1 (hERG) channels play a critical role in repolarization of cardiomyocytes during the cardiac action potential (AP). Drug mediated K_v11.1 blockade results in AP prolongation, which poses an increased risk of sudden cardiac death. Many drugs, like pentamidine, interfere with normal K_v11.1 forward trafficking and thus reduce functional K_v11.1 channel densities. Although class III antiarrhythmics, e.g. dofetilide, rescue congenital and acquired forward trafficking defects, this is of little use due to their simultaneous acute channel blocking effect. We aimed to test the ability of a combination of dofetilide plus LUF7244, a K_v11.1 allosteric modulator/activator, to rescue K_v11.1 trafficking and produce functional K_v11.1 current. LUF7244 treatment by itself did not disturb or rescue WT or G601S K_v11.1 trafficking as shown by western blot and immunofluorescence microscopy analysis. Pentamidine-decreased maturation of WT K_v11.1 levels was rescued by 10 μM dofetilide or 10 μM dofetilide + 5 μM LUF7244. In trafficking defective G601S K_v11.1 cells, dofetilide (10 μM) or dofetilide+LUF7244 (10+5 μM) restored K_v11.1 trafficking also, as demonstrated by western blot and immunofluorescence microscopy. LUF7244 (10 μM) increased I_{Kv11.1} despite the presence of dofetilide (1 μM) in WT K_v11.1 cells. In G601S expressing cells, long-term treatment (24-48 h) with LUF7244 (10 μM) and dofetilide (1 μM) increased I_{Kv11.1} compared to non-treated, or acutely treated cells. We conclude that dofetilide plus LUF7244 rescues K_v11.1 trafficking and produces functional I_{Kv11.1}. Thus, combined administration of

65 LUF7244 and an $I_{Kv11.1}$ trafficking corrector could serve as a new
66 pharmacological therapy of both congenital and drug-induced $K_v11.1$ trafficking
67 defects.

68

69 Key words: trafficking; $K_v11.1$; LUF7244; dofetilide; E4031; electrophysiology;
70 molecular dynamics

71 **Significance Statement**

72 LUF7244, a negative allosteric modulator/activator, in combination with
73 dofetilide corrected both congenital and acquired K_v11.1 trafficking defects
74 resulting in functional K_v11.1 current.

Introduction

Human K_v11.1 potassium ion channels (also known as hERG channels) stand at the basis of the rapidly activating delayed rectifier current (I_{Kr}) which is involved in phase three repolarization of the action potential (AP) in working cardiomyocytes (Vandenberg et al., 2012). Interference with normal I_{Kr} function can either shorten (gain-of-function) or prolong (loss-of-function) the process of ventricular repolarization as evident from QT-shortening or lengthening respectively, on the electrocardiogram (ECG) (Vandenberg et al., 2012). I_{Kr} inhibition in humans, e.g. by the class III agent dofetilide, is associated with life threatening ventricular arrhythmias (Torp-Pedersen et al., 1999). Fundamentally different mechanisms of I_{Kr} inhibition have been identified: 1) direct inhibition of potassium flow through the channel and 2) decreased plasma membrane expression of channel proteins, which both can result from mutations (*de novo* or congenital) or environmental factors (acquired, mostly drug-induced) (Sanguinetti and Tristani-Firouzi, 2006; De Gita et al., 2013). For these reasons, cardiac safety assessment of new chemical entities and preclinical drugs still has a strong focus on K_v11.1 channel function (Bossu et al., 2016) and mainly aims at detection of (semi)acute pore block. Interestingly, the far majority (approximately 90% of 167 tested) of congenital K_v11.1 loss-of-function missense mutations result in trafficking defects as a cause of I_{Kr} impairment (Anderson et al., 2006; 2016). For example, the G601S missense mutation in K_v11.1, located in the S5-pore helix linker, results in reduced

expression of functional I_{Kr} leading to hypomorphic LQT2 (Ficker et al., 2002). Also a number of drugs (>40% of 100 tested) limit expression of $K_v11.1$ at the plasma membrane by inhibiting its forward trafficking, with or without concomitant pore block (Wible et al., 2005). The anti-trypanosomiasis/leishmanias drug pentamidine is currently used as a $K_v11.1$ trafficking inhibitor without acute channel inhibition (Cordes et al., 2005; Kuryshv et al., 2005; Nalos et al., 2011; Himmel 2013; Varkevisser et al., 2013a, b; Obergrussberger et al., 2016). Pentamidine inhibits $K_v11.1$ forward trafficking at the level of endoplasmic reticulum exit in a process that involves the high affinity drug binding site F656 (Dennis et al., 2012). As a result, cells mainly express intracellularly localized core-glycosylated $K_v11.1$ with an apparent M_w of 135 kDa. High affinity $K_v11.1$ pore blockers such as E4031, dofetilide, cisapride and astemizole are able to rescue forward trafficking defects caused by either mutations or drugs (Zhou et al., 1999; Ficker et al., 2002; Varkevisser et al., 2013a; Yan et al., 2015). This will result in $K_v11.1$ maturation seen as a fully glycosylated protein with an apparent molecular weight of 155 kDa. The underlying mechanisms have not been clarified completely thus far, although it is found that channel inhibition potency correlates with rescue efficacy and that drug-channel interactions via high affinity binding sites are essential (Rajamani et al., 2002; Ficker et al., 2002; Dennis et al., 2012; Yan et al., 2015). Furthermore, EC_{50} values for rescue are generally much higher than IC_{50} values

119 for acute pore block (eg. Astemizole, IC_{50} =6-13 nM; EC_{50} for rescue=335±33
120 nM with 10 μ M pentamidine) (Ficker et al., 2002; Dennis et al., 2012).
121 Therefore, this strategy will not result in rescue of I_{Kr} function as long as the
122 high affinity blocker remains present whereas its withdrawal will not resolve the
123 underlying trafficking defects. Activators and negative allosteric modulators of
124 $K_v11.1$ have been developed as a strategy to counteract undesired I_{Kr} blockade
125 and thus potentially could “save” numerous (pre)clinical drugs with proven I_{Kr}
126 liability (Yu et al., 2014 and 2016; Sala et al., 2016; Qile et al., 2019). Allosteric
127 modulators interact with the $K_v11.1$ channel at a site different than that used by
128 the high affinity inhibitors, and thereby modulate binding affinities for the
129 canonical binding site of the latter. Activators interact with $K_v11.1$ at various
130 sites (Sanguinetti, 2014) and some share overlapping high affinity molecular
131 determinants (Casis et al, 2006; Perry et al, 2007; Garg et al, 2011) with
132 classical pore blockers. We have developed the negative allosteric
133 modulator/activator LUF7244 which indeed is able to counteract drug-induced
134 AP prolongation and proarrhythmia *in vitro* (Yu et al., 2015 and 2016) and drug-
135 induced ventricular arrhythmia *in vivo* (Qile et al., 2019). Specifically,
136 application of 10 μ M LUF7244 decreased the affinity of $K_v11.1$ for cisapride,
137 astemizole, dofetilide and sertindole by 4.0-, 3.8-, 3.2-, and 2.2-fold,
138 respectively (Yu et al., 2016). We hypothesized that LUF7244 would not
139 interfere in $K_v11.1$ trafficking by itself, and would also not interfere in dofetilide-

140 mediated rescue of defective forward trafficking, but maintains its ability to
141 increase I_{Kr} in the presence of dofetilide.

Materials and Methods

Chemicals

LUF7244 was custom synthesized at the Division of Drug Discovery and Safety, Leiden Academic Centre for Drug Research, Leiden University, The Netherlands as described earlier (Yu Z et al., 2016), dissolved in DMSO at 100 mM. Dofetilide was purchased from Sigma-Aldrich (Zwijndrecht, The Netherlands) and dissolved at 10 mM in DMSO. E4031 was dissolved in DMSO at 1 mM. Pentamidine-isethionate (Pentacarinat® 300, Sanofi Aventis, Gouda, The Netherlands) was dissolved in water to provide a stock solution of 100 mM. All compounds were sterilized by filtration (0.22 µm), aliquoted and stored at -20°C until use.

Molecular Modeling

Compounds LUF7244 and dofetilide were docked into the hERG cryo-EM structure (pdb code: 5va1, Wang and Mackinnon, 2017) using the GOLD software v.5.6.2. (Jones et al., 1997) essentially as described before (Qile et al., 2019). Two scoring functions ChemPLP and Goldscore were used and 100 poses collected per run with 125.000 Gold algorithm operations. The top 15 scoring poses each were analysed using PyMol 1.7.2 (Schrödinger, 2015).

Molecular dynamics Simulations

Simulations were essentially performed as described earlier (Qile et al., 2019) with few small modifications. The K_v11.1 hERG structure was embedded in a POPC bilayer and solvated with TIP3P water using the CHARMM-GUI (Jo et al., 2008). KCl (150 mM) was added to the system and potassium ions in the selectivity filter were placed at sites S0, S2 and S4, with water molecules at sites S1 and S3. Steepest descent energy minimization, followed by 2 ns equilibration and 50 ns production runs were performed using GROMACS v.5.1.2 (Abraham et al., 2015) and the charmm36 forcefield (Vanommeslaeghe et al., 2010). Electrostatics were modeled using Particle Mesh Ewald (Darden et al., 1993), and LINCS was used to constrain H-bonds (Hess et al., 1997). V-rescale (Bussi et al., 2007) was used to keep the temperature at 310 K, and semi-isotropic pressure coupling was done using the Parrinello-Rahman barostat (Parrinello and Rahman, 1981).

Cells

HEK-hERG cells which is the HEK293T cell line stably expressing human K_v11.1 protein, and hERG-G601S cells (HEK293T cell line stably expressing forward trafficking deficient K_v11.1 protein) were cultured in DMEM (Gibco-FisherScientific, Landsmeer, The Netherlands) supplemented with 10% fetal calf serum (Sigma-Aldrich, Zwijndrecht, the Netherlands), 2 mM L-glutamine, 50 U·mL⁻¹ penicillin, and 50 µg·mL⁻¹ streptomycin (all three Lonza, Breda, the Netherlands) as described before (Varkevisser et al., 2013a).

Patch clamp electrophysiology

HEK-hERG and hERG-G601S cells were grown on Ø12 mm glass cover slips coated with poly-L-lysine (Sigma-Aldrich, German) and placed in a perfusion chamber (Cell Microcontrols, Norfolk, VA, USA). Functional analyses were done by using standard whole-cell patch clamp technique on HEK293T cells stably expressing WT- or G601S-K_v11.1 channels. The external solution contained (mM): 137 NaCl, 4 KCl, 1.8 CaCl₂, 1 MgCl₂, 10 glucose and 10 HEPES (pH 7.4 adjusted with NaOH), and the internal pipette solution contained (mM): 130 KCl, 1 MgCl₂, 5 EGTA, 5 MgATP, 10 HEPES (pH 7.2 adjusted with KOH). An Axopatch-200B patch clamp amplifier (Axon Instruments, Union City, CA, USA) was used to measure macroscopic currents and cell capacitance. The pipette resistances were 1-3 MΩ and series resistance was compensated up to 90%. The pCLAMP 10 software (Axon Instruments) was used to generate the different voltage protocols, acquire current signals, and for data analyses. We determined the impact that dofetilide and LUF7244 had on K_v11.1 currents compared to control by applying step-like pulses from -80 mV to +60 mV in +10 mV increments for 5 s, followed by a “tail” pulse to -50 mV for 5 s. The maximal I_{Kv11.1} measured during the tail pulse was plotted as a function of the step-pulse potential to generate the corresponding I-V relations.

Western blot

Cell lysates were prepared in buffer D (20 mM HEPES, 125 mM NaCl, 10% glycerol, 1 mM EGTA, 1 mM dithiothreitol, 1 mM EDTA and 1% Triton X-100, pH 7.6) supplemented with 1 mM PMSF and 10 $\mu\text{g}\cdot\text{mL}^{-1}$ aprotinin. Twenty-five μg protein lysate was mixed with Laemmli sample buffer, separated by 7% SDS-PAGE and blotted onto a nitrocellulose membrane. Ponceau staining was used to reveal equal protein loading and subsequent quantification. Blots were blocked with 5% Protifar dissolved in TBST (20 mM Tris-HCl; pH 8.0, 150 mM NaCl, 0.05% Tween-20 (v/v)) for 1h at room temperature. K_v11.1 protein was detected by polyclonal anti-hK_v11.1 primary antibody (cat. no. APC-062; Alomone Labs, Jerusalem, Israel, 1:3000) and peroxidase-conjugated anti-rabbit secondary antibody (Jackson ImmunResearch Laboratories Inc., West Baltimore Pike West Grove, PA, USA; 1:10000). Final detection was performed using a standard ECL procedure (GE Lifescience, Marlborough, MA, USA) with ChemiDocXRS system (BioRad Laboratories, Veenendaal, The Netherlands). Quantification analysis was performed using Image J 1.48V software (National Institute of Health USA).

Immunofluorescence microscopy

HERG-G601S cells were grown on Ø 15 mm cover slips, coated with poly-L-Lysine, fixated with 3% paraformaldehyde dissolved in PBS containing 1 mM Ca²⁺ and 1 mM Mg²⁺, pH 7.4 for 20 minutes. Permeabilization was performed with 0.5% Triton X-100 in PBS for 3 minutes and 50 mM glycine-PBS was used

as quenching agent, cells were subsequently blocked with NET-gel (150 mM NaCl, 5 mM EDTA, 50 mM Tris-HCl, pH 7.4, 0.05% Igepal, 0.25% gelatin, 0.02% NaN₃). Then the cells were incubated with polyclonal anti-hK_v11.1 (1:3000, APC-062, Alomone Labs, Jerusalem, Israel) and anti-Pan-cadherin (1:800, Sigma-Aldrich, St Louis, MO, USA) primary antibody overnight in NET-gel, followed by incubation with secondary antibody of anti-mouse Alexa488 (Thermofisher Scientific) and anti-rabbit Alexa568 (Thermofisher Scientific, Landsmeer, The Netherlands) for 2h.

The cover slips were mounted with Vectashield (Vector Laboratories Inc. Burlingame, CA, USA), and fluorescent microscopy images were obtained using a Nikon ECLIPSE Ti2-E inverted microscope equipped with a ×60 oil immersion objective (NA 1.49) (CAIRN research, Faversham, UK). Excitation was performed with diode lasers (Omicron LuxX 488 nm 200mW for Alexa488 and an OBIS 561 nm 100mW for Alexa561). Colocalization between K_v11.1 and Cadherin in cell-extensions was quantified by determining Pearson's coefficient (r) with the Costes automated threshold method provided by the Coloc_2 plugin for the ImageJ software (1.52p) using Fiji.

Statistics

All averages values are expressed as mean ± standard deviation (SD), unless indicated otherwise. All statistical analyses were carried out by using SPSS version 21 and Graphpad Prism version 5. A difference was considered

252 significant with $P < 0.05$. Differences among groups were evaluated using either
253 one-way ANOVA with Dunnett's test for western blot and immunofluorescence
254 microscopy data or two-way ANOVA with Tukey's test for electrophysiology
255 data. Post hoc tests were carried out only if F was significant and there was no
256 variance in homogeneity.

Results

Docking and Molecular dynamics simulation-based prediction of binding mode of dofetilide and its interaction with LUF7244

Overview representations of K_v11.1 channel interaction with dofetilide and LUF7244 at the structural level, as viewed from the extracellular side, are shown in Figure 1A and Figure 1B. To investigate how LUF7244 might lower the channels affinities for dofetilide (Yu et al, 2016), we compared two binding modes of dofetilide and LUF7244. Figure 1C and D displays two alternative binding modes of dofetilide in the near-atomic resolution cryo-EM structure (3.4 Å) of the K_v11.1 K⁺ channel in agreement with experimental data: in the cavity, (Figure 1D), which is the classical assumed binding mode for blockers (Kamiya et al., 2006; Imai et al., 2009), or in the fenestrations, sticking into the cavity (Figure 1C), as suggested recently, based on hERG homology models (Saxena et al., 2016). Both binding modes can be recapitulated in docking studies to the cryo-EM structure and the drug is stable in 50 ns of Molecular dynamics (Figure 1G and H) in both sites. We have recently reported that LUF7244 might bind between the pore helices of two adjacent subunits, thereby stabilizing the conductive state of the channel (Qile et al, 2019). Comparison of the proposed binding modes of dofetilide with that of LUF7244 (Figure 1E and F) suggests that the allosteric negative inhibitor/activator could prevent the inhibitor from

binding to the fenestration site (Figure 1E), while there is almost no overlap, when dofetilide is bound to the central cavity (Figure 1F).

LUF7244 has no effect on K_v11.1 forward trafficking and does not interfere in dofetilide mediated rescue of pentamidine-induced trafficking defects

Application of LUF7244 (0.05, 0.1, 1, 3 and 5 μ M) for 48 h did not obviously affect K_v11.1 ratio of mature/immature protein as shown in Figure 2A. We demonstrated earlier that dofetilide rescues pentamidine-induced K_v11.1 forward trafficking defects (Varkevisser et al., 2013a). To determine if LUF7244 can restore mature K_v11.1 expression, different concentrations of LUF7244 were applied to HEK-hERG cells in the continuous presence of 10 μ M pentamidine. However, treatment with LUF7244 up to 5 μ M did not restore mature K_v11.1 protein levels (Figure 2B).

Since LUF7244 by itself could not restore normal forward K_v11.1 channel trafficking, did not affect trafficking by itself, and was found to counteract dofetilide-mediated I_{Kr} blockade (Qile et al., 2019), we questioned whether LUF7244 would influence dofetilide-mediated rescue of pentamidine induced trafficking defects. To test this hypothesis, the same dose range of LUF7244 was applied in combination with 1 μ M dofetilide and 10 μ M pentamidine for 48h. Interestingly, pentamidine decreased mature WT K_v11.1 protein (0.24 \pm 0.07 vs. 0.54 \pm 0.11 (control)), which was rescued by 1 μ M dofetilide (0.44 \pm 0.09 vs. 0.24 \pm 0.07) but also by the combination of 1 μ M dofetilide and 5 μ M LUF7244

(0.45±0.10 vs. 0.24±0.07) (Figure 2C). All the separate mature or immature K_v11.1 protein expression level, quantified from same blots, are shown in the right panel.

LUF7244 and dofetilide/E4031 rescue G601S-K_v11.1 maturation

In order to test the effects of LUF7244 on a congenital K_v11.1 loss-of-function missense mutation, which results in defective forward trafficking, we co-applied five different concentrations of LUF7244 and 1 μM dofetilide on hERG-G601S cells. According to western blot result, trafficking deficiency was observed which means only 135 kDa core-glycosylated immature protein was detected (Figure 3A). After 48 h administration of LUF7244 (0.05, 0.1, 1, 3 and 5 μM), mature K_v11.1 protein level was not changed compared with control (Figure 3A), whereas application of 1 μM dofetilide greatly increased mature protein expression. Furthermore, 1 μM dofetilide combined with LUF7244 (0.05-5 μM) also resulted in expression of the fully glycosylated mature protein (Figure 3B). To expand our findings to other I_{Kr} blockers, we used E4031. We applied 5 μM E4031 without or with LUF7244 (0.05, 0.1, 1, 3 and 5 μM) for 48h. Under all rescue conditions, the level of the 155 kDa fully glycosylated mature protein was increased (Figure 3C), although not to the same extent as seen with dofetilide. The separate mature or immature K_v11.1 protein expression level can be found in the right panel.

Immunofluorescence staining was used to determine the subcellular localization of the G601S-K_v11.1 protein. In untreated control hERG-G601S cells, no K_v11.1 protein was detected at the cell membrane structures such like membrane ruffles, in contrast to the transmembrane protein Cadherin (Figure 4) (Pearson coefficient of co-localization $r=0.20\pm0.35$, $n=6$). Following 24 h treatment with 10 μ M dofetilide or 10 μ M dofetilide+3 μ M LUF7244, normal trafficking was partly restored as evidenced by plasma membrane expression of K_v11.1 in membrane ruffles, where it colocalized with Cadherin (Figure 4) ($r=0.85\pm0.08$ ($n=6$) and 0.86 ± 0.06 ($n=6$), respectively, both $p<0.01$ vs. control or LUF7244). LUF7244 only treatment yielded no rescue of forward trafficking ($r=0.13\pm0.31$, n.s. vs. control). A lower concentration of LUF7244 was used to maintain intact cell structure in these experiments.

LUF7244 increases I_{KV11.1} in the presence of dofetilide

Lastly the impact of dofetilide and LUF7244 on I_{KV11.1} was determined (Figure 5). The use of 10 μ M LUF7244 in electrophysiology experiment is based on strong I_{KV11.1} blockade effect of dofetilide. To counteract dofetilide's effect, we needed to use relatively higher concentration than what we used in western blot experiments. On the other hand, 10 μ M LUF7244 was used in our previous work (Qile et al., 2019), which was based on the concentration that was used for its structural similar compound ICA-105574.

Figure 5A shows representative current traces measured from cells expressing WT-K_v11.1 channel proteins in control conditions or with application of dofetilide (1 μ M) or LUF7244 (10 μ M) or combination to the extracellular recording solution as acute treatment. Cells are voltage-clamped at a holding potential of -80 mV and depolarized to voltages between -80 and 60 mV for 5 s to activate I_{Kv11.1} (pre-pulse). The cells are then clamped to -50 mV for 5 s to record a tail current (test-pulses). As shown for control cells in Figure 5A, during depolarizing and tail pulses, an outward current was activated at voltages positive to -40 mV, and the current amplitude of the I_{Kv11.1} measured during the tail pulse increases with a maximum I_{Kv11.1} current following depolarizing pulses to >10 mV. The peak tail I_{Kv11.1} amplitude following repolarization was used to construct the activation curve shown in Figure 5B. The activation curve measured for control cells shows that the threshold voltage for I_{Kv11.1} activation is about -40 mV and that it is fully activated following voltage pulses to 10 mV. Dofetilide and LUF7244 dramatically alter the activation and kinetic properties of I_{Kv11.1}. The outward I_{Kv11.1} measured during the depolarization and tail pulses is larger than control from -70 mV to 10 mV; there is a negative shift in the corresponding I-V relation; but I_{Kv11.1} gets smaller following depolarizing pulses > 0 mV. The changes in the I_{Kv11.1} measured using this protocol in the presence of these drugs show complex changes consistent with both the activating properties of LUF7244 and blocking properties of dofetilide. The relevant LUF7244/dofetilide alone control study are shown in Figure 5.

Figure 6A shows representative current traces measured from cells expressing G601S-K_v11.1 channel proteins in control conditions and with acute or long-term application of dofetilide+LUF7244, or LUF7244 only to the extracellular recording solution. There was no statistical difference in I_{Kv11.1} between the control conditions and acute application of dofetilide + LUF7244. Therefore, we tested the long-term effects of these drugs on I_{Kv11.1}. We incubated cells in dofetilide + LUF7244 for 24-48 h and then recorded I_{Kv11.1} from cells with these drugs in the extracellular recording solution. The mean I-V relations, based on peak tail I_{Kv11.1} amplitude following repolarization, for cells expressing G601S-K_v11.1 channel proteins in the different conditions indicate that long-term dofetilide + LUF7244 treatment increased I_{Kv11.1}. Dofetilide only treatment had a minimal effect (Figure 6B) indicating the presence of only few functional channels at the plasma membrane without prior pharmacological correction of trafficking. Interestingly however, LUF7244 only treatment produced I_{Kv11.1} under such condition (Figure 6A, B). Compared to control cells: cells cultured and recorded in dofetilide + LUF7244 increased I_{Kv11.1} following pre-pulses to -40mV to 60 mV (p<0.05), and cells treated with LUF7244 increased I_{Kv11.1} following pre-pulses from -80mV to 60mV (p<0.05). Compared to cells recorded in dofetilide: cells cultured and recorded in dofetilide + LUF7244 increased I_{Kv11.1} following pre-pulses to -40mV to 60 mV (p<0.05), and cells recorded in LUF7244 increased I_{Kv11.1} following pre-pulses from -80mV to 60mV (p<0.05). Compared to cells recorded in dofetilide + LUF7244: cells cultured and

386 recorded in dofetilide + LUF7244 increased $I_{Kv11.1}$ following pre-pulses to -30mV
387 to 30 mV ($p<0.05$), and cells recorded in LUF7244 increased $I_{Kv11.1}$ following
388 pre-pulses from -80mV to 60mV ($p<0.05$). Compared to cells cultured and
389 recorded in LUF7244 cells, cells recorded in LUF7244 increased $I_{Kv11.1}$ following
390 pre-pulses from -80mV to 60mV ($p<0.05$).

Discussion

K_v11.1 activators and negative allosteric modulators use mechanistically different ways to increase or maintain normal I_{Kr} levels in the presence of a K_v11.1 channel inhibitor. A number of compounds have been demonstrated as K_v11.1 activators (Perry et al., 2010). Activators influence gating kinetics and can for example slow down or remove inactivation and/or facilitate activation (Sanguinetti, 2014). K_v11.1 activators normally interact with a region distant from the inner cavity (Perry et al., 2010) but they can bind to several distinct sites of the channel (Guo et al, 2015; Perry et al, 2007; Gardner et al 2017). Negative allosteric modulators decrease the binding affinity of I_{Kr} blockers, either by increasing dissociation rates, lowering association rates or both (Christopoulos et al., 2014). In our previous study, and also shown here, LUF7244 alone can dose-dependently increase K_v11.1 current and reduce inactivation of K_v11.1 at higher concentration (Qile et al., 2019). In the current study, instead of the blockade effect of dofetilide, dofetilide+LUF7244 treatment statistically significant increased I_{Kv11.1} level in HEK-hERG cell. In G601S cells, dofetilide+LUF7244 treatment increased (not statistically significantly) steady state current as well. Furthermore, long term exposure increased I_{Kv11.1} continuously. It indicates that I_{Kr} inhibitors acute channel blockade could be reversed by LUF7244. And its trafficking rescue characteristic might further functionally benefits K_v11.1 for long term administration.

We observed a stronger $I_{Kv11.1}$ increase for G601S channels than for WT channels (Figure 5, 6) which could not be explained by methodological means. Although speculative, we can envision that besides an effect on trafficking, the G601S mutation may result in increased binding affinity for LUF7244, or show subtle differences channel kinetics in response to LUF7244 compared to WT. Whether these effects are mutation specific are points for further investigation. Furthermore, the finding that LUF7244 can strongly activate the low amount of G601S channels that do reach the plasma membrane in cells not treated with dofetilide, may shortcut the need for complete restoration of trafficking.

Modeling suggests that LUF7244 disrupts drug block at the fenestration, via binding close to the protein-lipid interface (Figure 1F). Drug binding to this site has recently been reported for Ivabradine, a low μ molar affinity $K_v11.1$ blocker (Perissinotti et al., 2019). It has been reported that this drug interacts with lipid-facing residues in the fenestration, including F557 and F656, in a state-dependent manner. Even though, dofetilide is unlikely to access the $K_v11.1$ cavity, via this fenestration, as has been shown for the more lipophilic drug Ivabradine, residue F557 has been shown to reduce binding affinity > 50-fold, when mutated to a leucine (Saxena et al., 2016). This suggests that this lipid-facing residue is critical for high affinity block of different hERG inhibitors. Our modeling proposes that LUF7244 could disrupt coupling between state-dependent dynamics of F557 and F656 and interfere with dofetilide binding to the fenestration (Figure 1E). Given the impact of LUF7244 on inactivation, one

plausible scenario would be that the negative allosteric inhibitor prevents dofetilide from binding or accessing the “high affinity” inactivated state in the fenestration, but this will require further modeling of the inactivated state(s). However, based on the current simulations of 50 ns, we cannot exclude that $K_v11.1$ has additional LUF7244 binding sites. Additional binding sites may explain the dual character of LUF7244 as a negative allosteric modulator (Yu et al., 2016) and activator (Qile et al., 2019, this study). Additional experimental analyses that may require in depth NMR studies on drug-channel interaction deem necessary to resolve this issue. The I_{Kr} activator ICA-105574 has structural similarities with LUF7244, and has also similar functional characteristics (Gerlach et al., 2010). It was shown that ICA-105574 enhanced $K_v11.1$ currents via a mechanism that seems to prevent or limit the inactivation gating process. Additionally, ICA-105574 dose dependently shortened the AP duration in isolated guinea pig ventricular cardiomyocytes. It also remarkably suppressed the $K_v11.1$ channel inhibitor E4031-induced AP lengthening. In this perspective, it would be interesting to compare these two compounds with respect to the mechanism of action on $K_v11.1$ channels. Besides, in view of its predicted binding site, LUF7244 by itself had no effects on $K_v11.1$ channel trafficking, neither did it inhibit pentamidine-associated trafficking defects nor did it affect dofetilide-mediated rescue. Previously, we demonstrated that pentamidine-induced $K_v11.1$ forward trafficking defects could be rescued by dofetilide and both compounds may compete for the same

456 binding site within the K_v11.1 channel (Varkevisser et al., 2013a). Defective
457 K_v11.1 forward trafficking can be restored by a number of K_v11.1 inhibitors that
458 stabilize the channel via binding to the inner pore, close to the selectivity filter
459 (e.g. Varkevisser et al., 2013a; Perry et al., 2010). We demonstrated that
460 dofetilide analogues with higher affinity tended to provide better rescue in
461 K_v11.1 trafficking defects, while LUF7244 reduced the K_v11.1 channel affinity
462 for dofetilide (Yu et al., 2016). Interestingly, in our current study, the
463 combination of dofetilide and LUF7244 still rescued pentamidine induced
464 K_v11.1 trafficking defects. One possible reason may be that LUF7244 can not
465 completely reduce the binding of dofetilide to the trafficking inhibited channels
466 by which the capacity of dofetilide to rescue K_v11.1 trafficking remained.
467 Another possibility is the absence of LUF7244 binding to intracellularly localized,
468 immature and only core-glycosylated K_v11.1 channels. This may also explain 1)
469 the absence of effects of LUF7244 on defective G601S trafficking, 2) lack of
470 interference of pentamidine-mediated trafficking defects by LUF7244, and 3)
471 permitting dofetilide- and E4031-mediated rescue of K_v11.1 trafficking. Recent
472 preliminary data indicate that dofetilide specifically binds to membrane
473 preparations of G601S cells, which is in line with the observed trafficking rescue
474 effect. It now has to be determined to which extent this binding is sensitive to
475 LUF7244. We hypothesize that LUF7244 will certainly not completely inhibit
476 dofetilide binding to intracellularly localized K_v11.1, otherwise

dofetilide+LUF7244 would not provide any rescue of maturation, membrane staining and $I_{Kv11.1}$ as shown in the current manuscript.

Negative allosteric modulators and activators can be considered as therapeutic options to prevent drug-induced arrhythmia (Sanguinetti 2014; Yu et al, 2016). Recently, we have shown that LUF7244 suppressed astemizole-induced early after depolarizations (EADs) and AP prolongation in neonatal rat ventricular myocytes (NRVM) (Yu et al., 2016). Additionally, LUF7244 pretreatment prevented the occurrence of astemizole induced EADs, while LUF7244 per se did not shorten AP duration or strongly affect dispersion of APD_{40} in NRVM at 10 μ M (Yu Z et al., 2016). In contrast, in isolated canine ventricular cardiomyocytes and human iPS-derived cardiomyocytes, LUF7244 remarkably shortened the APD_{90} , which is in line with its activator characteristics (Qile et al., 2019). Moreover, we demonstrated that LUF7244 suppressed EADs in isolated canine ventricular myocytes and prevented dofetilide-induced ventricular arrhythmias in the dog with chronic AV block (Qile et al., 2019).

In conclusion, the current study demonstrates that LUF7244, and possibly also other negative allosteric modulators and activators, might also have a role in suppression or preventing arrhythmia caused by defective forward trafficking. Thus, the negative allosteric modulator/activator LUF7244 in combination with

498 a genuine K_v11.1 inhibitor could provide a new pharmacological treatment to
499 functionally correct both congenital and acquired K_v11.1 trafficking defects.

500 **Acknowledgments**

501 The authors thank Jacobus P. van Veldhoven from Leiden University for the
502 synthesis of LUF7244.

503 **Authorship contributions**

504 Participated in research design: Heyden, Stry, Delisle

505 Conducted experiments: Qile, Ji, Golden, Houtman, Romunde, Fransen, Ham

506 Contributed to reagents or analytic tools: IJerman, January, Heitman, Stry,

507 Delisle

508 Performed data analysis: Qile, Ji, Golden, Houtman, Ham

509 Wrote or contributed to the writing of the manuscript: Heyden, Ji, Qile, Stry,

510 Delisle

511 Critical review and approval of final manuscript: all authors

References

Abraham M, Hess B, van der Spoel D, and Lindahl E (2015). USER MANUAL Version 5.0. 7. The GROMACS Development Teams at the Royal Institute of Technology and Uppsala University, Sweden.

Anderson CL, Delisle BP, Anson BD, Kilby JA, Will ML, Tester DJ, Gong Q, Zhou Z, Ackerman MJ, and January CT (2006) Most LQT2 mutations reduce K_v11.1 (hERG) current by a class 2 (trafficking-deficient) mechanism. *Circulation* **113**:365-373.

Anderson CL, Kuzmicki CE, Childs RR, Hintz CJ, Delisle BP, and January CT (2016) Large-scale mutational analysis of K_v11.1 reveals molecular insights into type 2 long QT syndrome. *Nat Commun* **5**:5535.

Bossu A, van der Heyden MAG, de Boer TP, and Vos MA (2016) A 2015 focus on preventing drug-induced arrhythmias. *Expert Rev Cardiovasc Ther* **14**:245-253.

Bussi G, Donadio D, and Parrinello M (2007) Canonical sampling through velocity rescaling. *J Chem Phys* **126**:014101.

- 532 Casis O, Olesen SP, and Sanguinetti MC (2006) Mechanism of action of a novel
533 human ether-a-go-go-related gene channel activator. *Mol Pharmacol*, **69**:658-
534 665.
- 535
- 536 Christopoulos A, Changeux JP, Catterall WA, Fabbro D, Burris TP, Cidlowski
537 JA, Olsen RW, Peters JA, Neubig RR, Pin JP, and Sexton PM (2014) Multisite
538 pharmacology: recommendations for the nomenclature of receptor allosterism
539 and allosteric ligands. *Pharmacol Rev* **66**:918-947.
- 540
- 541 Cordes JS, Sun Z, Lloyd DB, Bradley JA, Opsahl AC, Tengowski MW, Chen X,
542 and Zhou J (2005) Pentamidine reduces hERG expression to prolong the QT
543 interval. *Br J Pharmacol* **145**:15-23.
- 544
- 545 Darden T, York D, and Pedersen L (1993) Particle mesh Ewald: An $N \cdot \log(N)$
546 method for Ewald sums in large systems. *J Chem Phys* **98**:10089-10092.
- 547
- 548 De Git KC, de Boer TP, Vos MA, and van der Heyden MAG (2013) Cardiac ion
549 channel trafficking defects and drugs. *Pharmacol Ther* **139**:24-31.
- 550
- 551 Dennis AT, Wang L, Wan H, Nassal D, Deschenes I, and Ficker E (2012)
552 Molecular determinants of pentamidine-induced hERG trafficking inhibition. *Mol*
553 *Pharmacol* **81**:198-209.

554

555 Ficker E, Obejero-Paz CA, Zhao S, and Brown AM (2002) The binding site for
556 channel blockers that rescue misprocessed human long QT syndrome type 2
557 ether-a-gogo-related gene (HERG) mutations. *J Biol Chem* **277**:4989-4998.

558

559 Gardner A, Wu W, Thomson S, Zangerl-Plessl EM, Stary-Weinzinger A, and
560 Sanguinetti MC (2017) Molecular Basis of Altered hERG1 Channel Gating
561 Induced by Ginsenoside Rg3. *Mol Pharmacol* **92**:437-450.

562

563 Garg V, Stary-Weinzinger A, and Sanguinetti MC (2013) ICA-105574 interacts
564 with a common binding site to elicit opposite effects on inactivation gating of
565 EAG and ERG potassium channels. *Mol Pharmacol* **83**:805-813.

566

567 Gerlach AC, Stoehr SJ, and Castle NA (2010) Pharmacological removal of
568 human ether-a-go-go-related gene potassium channel inactivation by 3-nitro-
569 N-(4-phenoxyphenyl) benzamide (ICA-105574). *Mol Pharmacol* **77**:58-68.

570

571 Guo J, Cheng YM, Lees-Miller JP, Perissinotti LL, Claydon TW, Hull CM,
572 Thouta S, Roach DE, Durdagi S, Noskov SY, and Duff HJ (2015) NS1643
573 interacts around L529 of hERG to alter voltage sensor movement on the path
574 to activation. *Biophys J* **108**:1400-1413.

575

576 Hess B, Bekker H, Berendsen HJC, and Fraaije JGEM (1997) LINCS: a linear
577 constraint solver for molecular simulations. *J Comput Chem* **18**:1463-1472.

578

579 Himmel HM (2013) Drug-induced functional cardiotoxicity screening in stem
580 cell-derived human and mouse cardiomyocytes: effects of reference
581 compounds. *J Pharmacol Toxicol Methods* **68**:97-111.

582

583 Imai YN, Ryu S, and Oiki S (2009) Docking model of drug binding to the human
584 ether-a-go-go potassium channel guided by tandem dimer mutant patch-clamp
585 data: a synergic approach. *J Med Chem* **52**:1630-1638.

586

587 Jones G, Willett P, Glen RC, Leach AR, and Taylor R (1997) Development and
588 validation of a genetic algorithm for flexible docking. *J Mol Biol* **267**:727-748.

589

590 Jo S, Kim T, Iyer VG, and Im W (2008) CHARMM-GUI: a web-based graphical
591 user interface for CHARMM. *J Comput Chem* **29**:1859-1865.

592

593 Kamiya K, Niwa R, Mitcheson JS, and Sanguinetti MC (2006) Molecular
594 determinants of HERG channel block. *Mol Pharmacol* **69**:1709-1716.

595

- 596 Kuryshev YA, Ficker E, Wang L, Hawryluk P, Dennis AT, Wible BA, Brown AM,
597 Kang J, Chen XL, Sawamura K, Reynolds W, and Rampe D (2005)
598 Pentamidine-induced long QT syndrome and block of hERG trafficking. *J*
599 *Pharmacol Exp Ther* **312**:316-323.
- 600
- 601 Nalos L, de Boer TP, Houtman MJ, Rook MB, Vos MA, and van der Heyden
602 MAG (2011) Inhibition of lysosomal degradation rescues pentamidine-mediated
603 decreases of K_{IR}2.1 ion channel expression but not that of K_V11.1. *Eur J*
604 *Pharmacol* **652**:96-103.
- 605
- 606 Obergrussberger A, Juhasz K, Thomas U, Stölzle-Feix S, Becker N, Dörr L,
607 Beckler M, Bot C, George M, and Fertig N (2016) Safety pharmacology studies
608 using EFP and impedance. *J Pharmacol Toxicol Methods* **81**:223-232.
- 609
- 610 Parrinello M, and Rahman A (1981) Polymorphic transitions in single crystals:
611 A new molecular dynamics method. *J Appl Phys* **52**:7182-7190.
- 612
- 613 Perissinotti L, Guo J, Kudaibergenova M, Miller JL, Khovich MO, Sharapova A,
614 Perlovich G, Muruve D, Gerull B, Noskov SY, and Duff HJ (2019) The Pore-
615 Lipid Interface: Role of Amino Acid Determinants of Lipophilic Access by
616 Ivabradine to the hERG1 Pore Domain. *Mol Pharmacol* **96**:259-271.

617

618 Perry M, Sachse FB, and Sanguinetti MC (2007) Structural basis of action for
619 a human ether-a-go-go-related gene 1 potassium channel activator. *Proc Natl*
620 *Acad Sci U S A* **104**:13827-13832.

621

622 Perry M, Sanguinetti M, and Mitcheson J (2010) Symposium review: Revealing
623 the structural basis of action of hERG potassium channel activators and
624 blockers. *J Physiol* **588**:3157-3167.

625

626 Qile M, Beekman HD, Sprenkeler DJ, Houtman MJ, van Ham WB, Stary-
627 Weinzinger A, Beyl S, Hering S, van den Berg DJ, de Lange EC, Heitman LH,
628 IJzerman AP, Vos MA, and van der Heyden MA (2019) LUF7244, an allosteric
629 modulator/activator of K_v11.1 channels, counteracts dofetilide-induced TdP
630 arrhythmia in the chronic atrioventricular block dog model. *Br J Pharmacol*
631 **176**:3871-3885.

632

633 Rajamani S, Anderson CL, Anson BD, and January CT (2002) Pharmacological
634 rescue of human K⁺ channel long-QT2 mutations: human ether-a-go-go-related
635 gene rescue without block. *Circulation* **105**:2830-2835.

636

637 Sala L, Yu Z, Ward-van Oostwaard D, van Veldhoven JP, Moretti A, Laugwitz
638 KL, Mummery CL, IJzerman AP, and Bellin M (2016) A new hERG allosteric

639 modulator rescues genetic and drug-induced long-QT syndrome phenotypes in
640 cardiomyocytes from isogenic pairs of patient induced pluripotent stem
641 cells. *EMBO Mol Med* **8**:1065-1081.

642

643 Sanguinetti MC (2014) HERG1 channel agonists and cardiac arrhythmia. *Curr*
644 *Opin Pharmacol* **15**:22-27.

645

646 Sanguinetti MC and Tristani-Firouzi M (2006) hERG potassium channels and
647 cardiac arrhythmia. *Nature* **440**:463-469.

648

649 Saxena P, Zangerl-Plessl EM, Linder T, Windisch A, Hohaus A, Timin E, Hering
650 S, and Stry-Weinzinger A (2016) New potential binding determinant for hERG
651 channel inhibitors. *Sci Rep* **6**:24182.

652

653 Schrodinger, LLC (2015) The PyMOL molecular graphics system, version
654 1.8. *Schrodinger LLC, New York, NY*.

655

656 Torp-Pedersen C, Møller M, Bloch-Thomsen PE, Køber L, Sandøe E, Egstrup
657 K, Agner E, Carlsen J, Videbaek J, Marchant B, and Camm AJ (1999) Dofetilide
658 in patients with congestive heart failure and left ventricular dysfunction. *N Engl*
659 *J Med* **341**:857-865.

660

- 661 Vandenberg JI, Perry MD, Perrin MJ, Mann SA, Ke Y, and Hill AP (2012) hERG
662 K⁺ channels: structure, function, and clinical significance. *Physiol Rev* **92**:1393-
663 1478.
- 664
- 665 Vanommeslaeghe K, Hatcher E, Acharya C, Kundu S, Zhong S, Shim J, Darian
666 E, Guvench O, Lopes P, Vorobyov I, and MacKerell Jr AD (2010) CHARMM
667 general force field: A force field for drug-like molecules compatible with the
668 CHARMM all-atom additive biological force fields. *J Comput Chem* **31**:671-690.
- 669
- 670 Varkevisser R, Houtman MJ, Linder T, de Git KC, Beekman HD, Tidwell RR,
671 IJzerman AP, Stary-Weinzinger A, Vos MA, and van der Heyden MAG (2013a)
672 Structure-activity relationships of pentamidine-affected ion channel trafficking
673 and dofetilide mediated rescue. *Br J Pharmacol* **169**:1322-1334.
- 674
- 675 Varkevisser R, Houtman MJ, Waasdorp M, Man JC, Heukers R, Takanari H,
676 Tieland RG, van Bergen en Henegouwen PM, Vos MA, and van der Heyden
677 MAG (2013b) Inhibiting the clathrin-mediated endocytosis pathway rescues
678 K_{IR}2.1 downregulation by pentamidine. *Pflugers Arch* **465**:247-259.
- 679
- 680 Wang W and MacKinnon R (2017) Cryo-EM structure of the open human ether-
681 à-go-go-related K⁺ channel hERG. *Cell* **169**:422-430.
- 682

683 Wible BA, Hawryluk P, Ficker E, Kuryshv YA, Kirsch G, and Brown AM (2005)
684 HERG-Lite: a novel comprehensive high-throughput screen for drug-induced
685 hERG risk. *J Pharmacol Toxicol Methods* **52**:136-145.
686
687 Yan M, Zhang K, Shi Y, Feng L, Lv L, and Li B (2015) Mechanism and
688 pharmacological rescue of berberine-induced hERG channel deficiency. *Drug*
689 *Des Devel Ther* **9**:5737-5747.
690
691 Yu Z, Klaasse E, Heitman LH, and IJzerman AP (2014) Allosteric modulators
692 of the hERG K⁺ channel: radioligand binding assays reveal allosteric
693 characteristics of dofetilide analogs. *Toxicol Appl Pharmacol* **274**:78-86.
694
695 Yu Z, Liu J, van Veldhoven JP, IJzerman AP, Schlij MJ, Pijnappels DA,
696 Heitman LH, and de Vries AA (2016) Allosteric Modulation of Kv11.1 (hERG)
697 Channels Protects Against Drug-Induced Ventricular Arrhythmias. *Circ*
698 *Arrhythm Electrophysiol* **9**:e003439.
699
700 Yu Z, van Veldhoven JP, 't Hart IM, Kopf AH, Heitman LH, and IJzerman AP
701 (2015) Synthesis and biological evaluation of negative allosteric modulators of
702 the Kv11.1 (hERG) channel. *Eur J Med Chem* **106**:50-59.
703

704 Zhou Z, Gong Q, and January CT (1999) Correction of defective protein
705 trafficking of a mutant HERG potassium channel in human long QT syndrome.
706 Pharmacological and temperature effects. *J Biol Chem* **274**:31123-31126.
707

708 **Footnotes**

709 This work was supported by the Chinese Scholarship Council; The Netherlands

710 Heart Foundation [travel grant 2018SB002].

711 Part of this abstract has been presented at the 41st meeting of the ESC Working

712 Group on Cardiac Cellular Electrophysiology, June 17–19, 2017, Vienna,

713 Austria

Figure legends

Figure 1

Molecular dynamics simulation-based prediction of binding mode of dofetilide/LUF7244 and K_v11.1. (A) Overview of the hERG structure (top view), with bound dofetilide at the fenestration, shown as orange spheres. (B) Overview of the hERG structure (top view), with bound LUF7244. (C) Predicted binding modes for dofetilide at the fenestration. (D) Predicted 'classical' binding mode for dofetilide in the inner cavity of hERG. Yellow dotted lines indicate putative π - π interactions; red dotted lines indicate H-bonds. (E) and (F) superposition of dofetilide binding modes, with predicted LUF7244 binding mode. (G) and (H) Root mean square deviation (RMSD) of K_v11.1 and dofetilide docked into the fenestration or cavity, respectively.

Figure 2

LUF7244 alone has no effect on K_v11.1 trafficking and does not disturb dofetilide-mediated rescue of forward trafficking. (A) Western blot showing that treatment of pentamidine-exposed (10 μ M, 48 h) HEK-hERG cells with 1 μ M dofetilide restored mature K_v11.1 expression. LUF7244 alone has no effect on K_v11.1 expression (n=3). Mature (plasma membrane expressed) and immature (intracellular) K_v11.1 western blot signals are displayed in left panel. Bar graphs in the middle depict ratio of mature/immature K_v11.1 at different conditions. The

right panel displays separate values for mature and immature K_v11.1. (B) LUF7244 does not rescue pentamidine-induced K_v11.1 trafficking defects (n=3). (C) Combination of pentamidine, dofetilide and LUF7244 restores K_v11.1 mature protein after 48 h (n=6). Total protein staining (Ponceau) was used as a loading control. *** $P < 0.001$, **** $P < 0.0001$ vs. control. Values are shown as mean \pm SD. One-way ANOVA with Dunnett's test was applied for group comparison.

Figure 3

LUF7244 combined with dofetilide or E4031 rescues trafficking defective K_v11.1-G601S maturation. (A) Western blot analysis of equal amounts (25 μ g) of total protein from K_v11.1-G601S cells. G601S cells only present a core-glycosylated immature protein of 135 kDa. Dofetilide restores expression of the full-glycosylated mature protein after 48 h. LUF7244 does not change the mature K_v11.1 protein levels compared with control (n=3). (B) The combination of dofetilide and LUF7244 rescues mature K_v11.1 protein in G601S cells (n=3). (C) Increased mature K_v11.1 levels in G601S cells treated with E4031 or E4031+LUF7244 (48h) (n=6). The right panel displays separate values for mature and immature K_v11.1. Total protein staining (Ponceau) was used as a loading control. * $P < 0.05$, ** $P < 0.01$, *** $P < 0.001$ vs. control. Values are shown as mean \pm SD. One-way ANOVA with Dunnett's test was applied for group comparison.

Figure 4

G601S cells were either non-treated (control), treated with 10 μ M Dofetilide, 3 μ M LUF7244, or 10 μ M Dof+3 μ M LUF for 24 hours. K_v11.1 channels were labelled (left column) along with Cadherin as a pseudo-membrane marker (Cadherin). Linescans of selected regions at cell extensions (containing membrane ruffles) are indicated in the merged pictures by boxes. Results of the linescan recordings are given on the right panels. Scale bar represents 10 μ m.

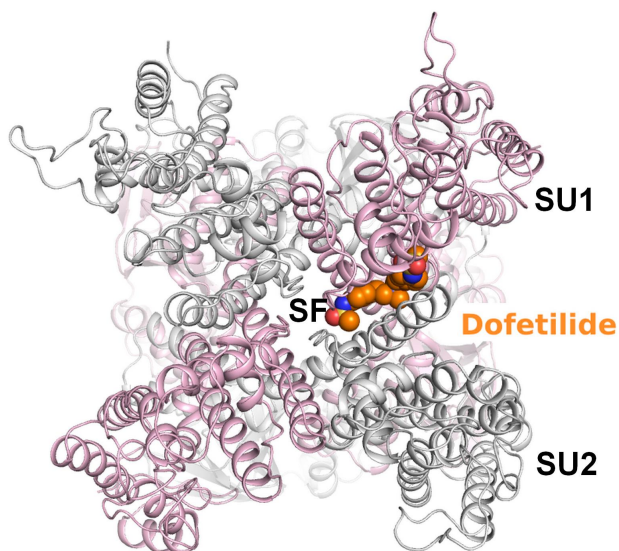
Figure 5

LUF7244 combined with dofetilide acutely rescued I_{Kv11.1} in HEK-hERG cells. (A) Shown are representative currents from cells expressing WT-K_v11.1 channel proteins using the voltage protocol in the inset. Cells were recorded in control conditions or in dofetilide + LUF7244 (acute application). In B shown are the mean I-V relations, based on peak tail I_{Kv11.1} amplitude following repolarization, recorded from cells expressing WT-K_v11.1 channel proteins. Cells were recorded in control conditions (n = 10) or in dofetilide + LUF7244 (acute) (n = 10). Data are shown as mean \pm SEM. Compared to control cells, cells recorded in dofetilide + LUF7244 increased I_{Kv11.1} following pre-pulses from -70mV to 10 mV (p<0.05). Two-way ANOVA with Tukey's test was applied.

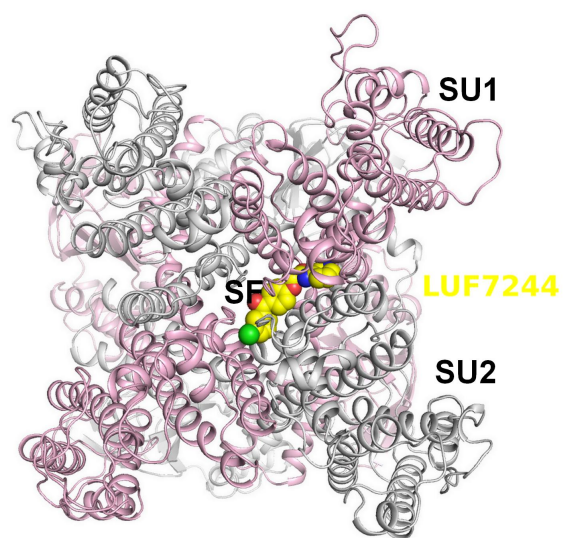
Figure 6

Long-term (24-48h) exposure of LUF7244 combined with dofetilide rescued $I_{Kv11.1}$ in G601S cells. (A) Shown are representative currents from cells expressing G601S- $K_v11.1$ channel proteins using the voltage protocol in the inset. Cells were recorded in control conditions, in dofetilide + LUF7244 (acute), in dofetilide + LUF7244 after being cultured in dofetilide + LUF7244 for long-term (LT), or in LUF7244 (acute). (B) Shown are the mean I-V relations, based on peak tail $I_{Kv11.1}$ amplitude following repolarization, recorded from cells expressing G601S- $K_v11.1$ channel proteins. Cells were recorded in control conditions (n = 10), in dofetilide (n = 8), dofetilide + LUF7244 (acute) (n = 10), in dofetilide + LUF7244 after being cultured in dofetilide + LUF7244 for 24-48 hours (LT) (n = 10), or in LUF7244 (n = 7). Data are shown as mean \pm SEM. Two-way ANOVA with Tukey's test was applied.

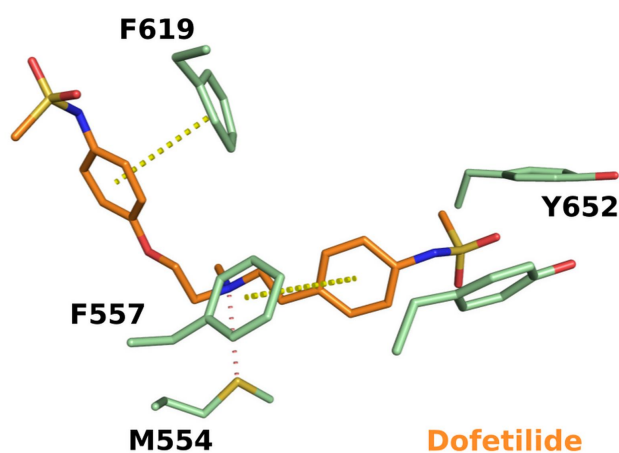
A



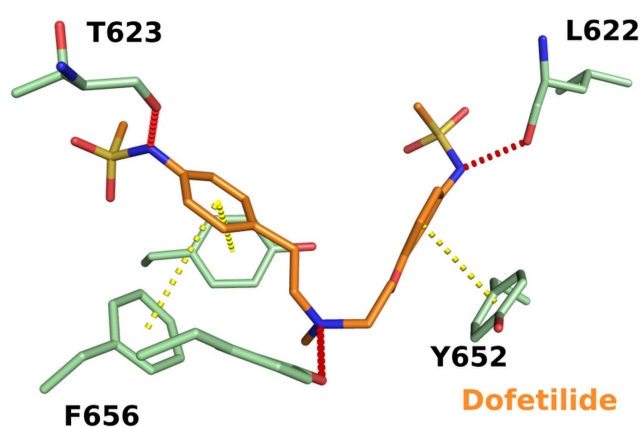
B



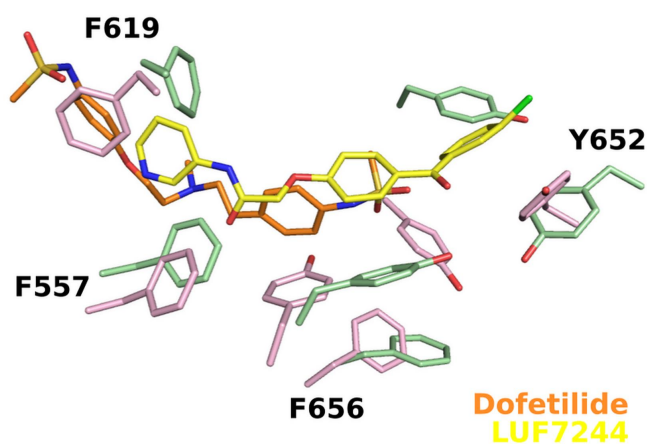
C



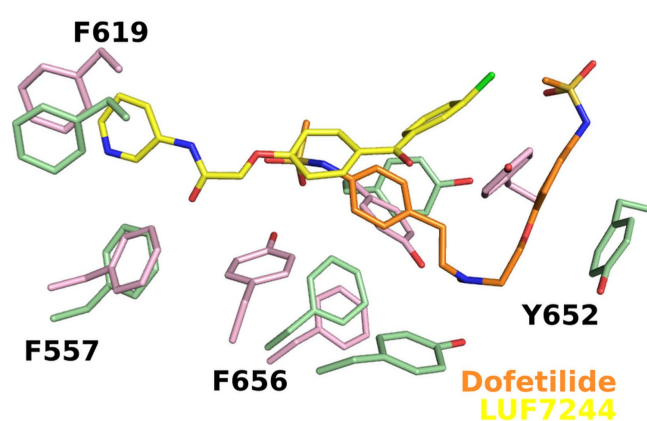
D



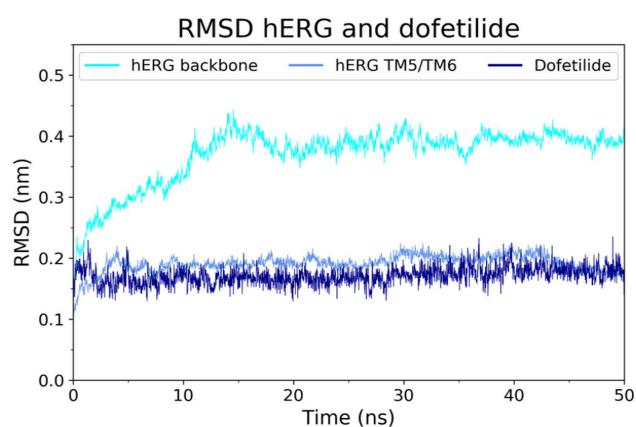
E



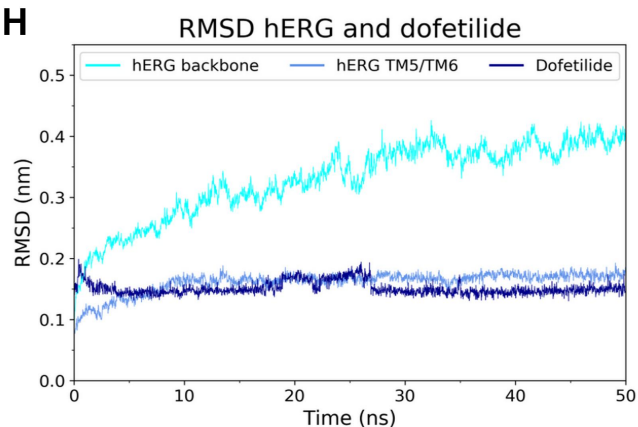
F



G



H



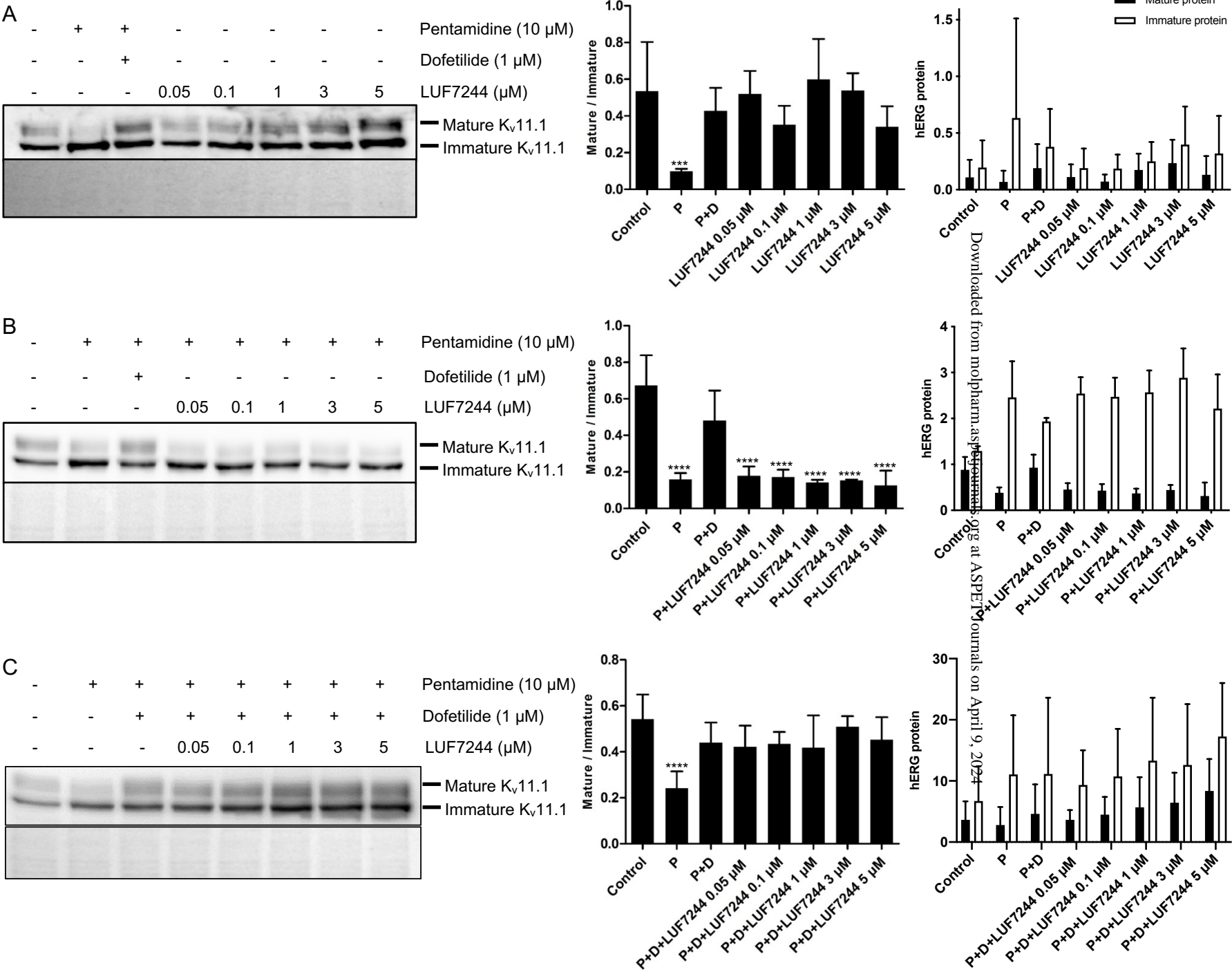


Figure 2

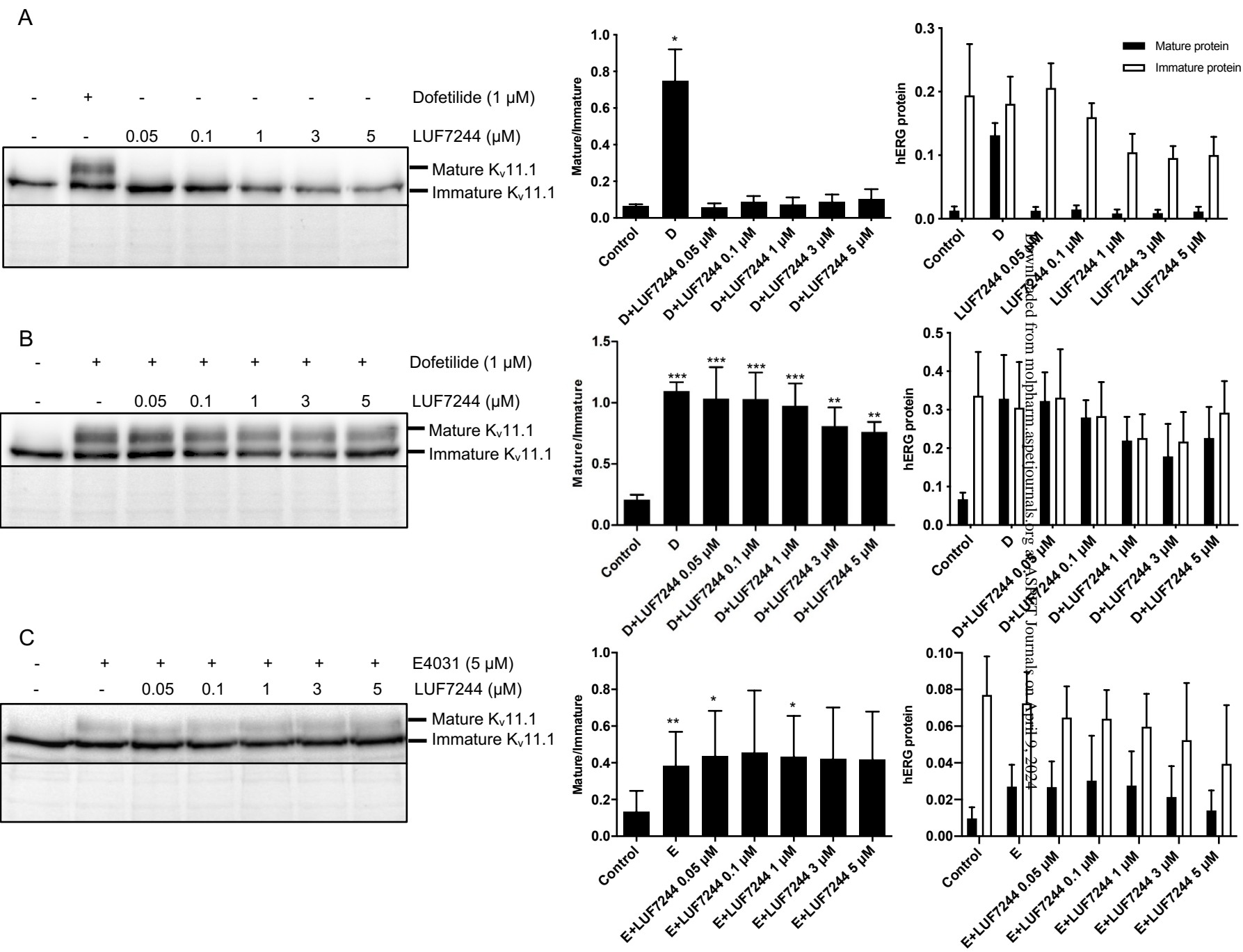
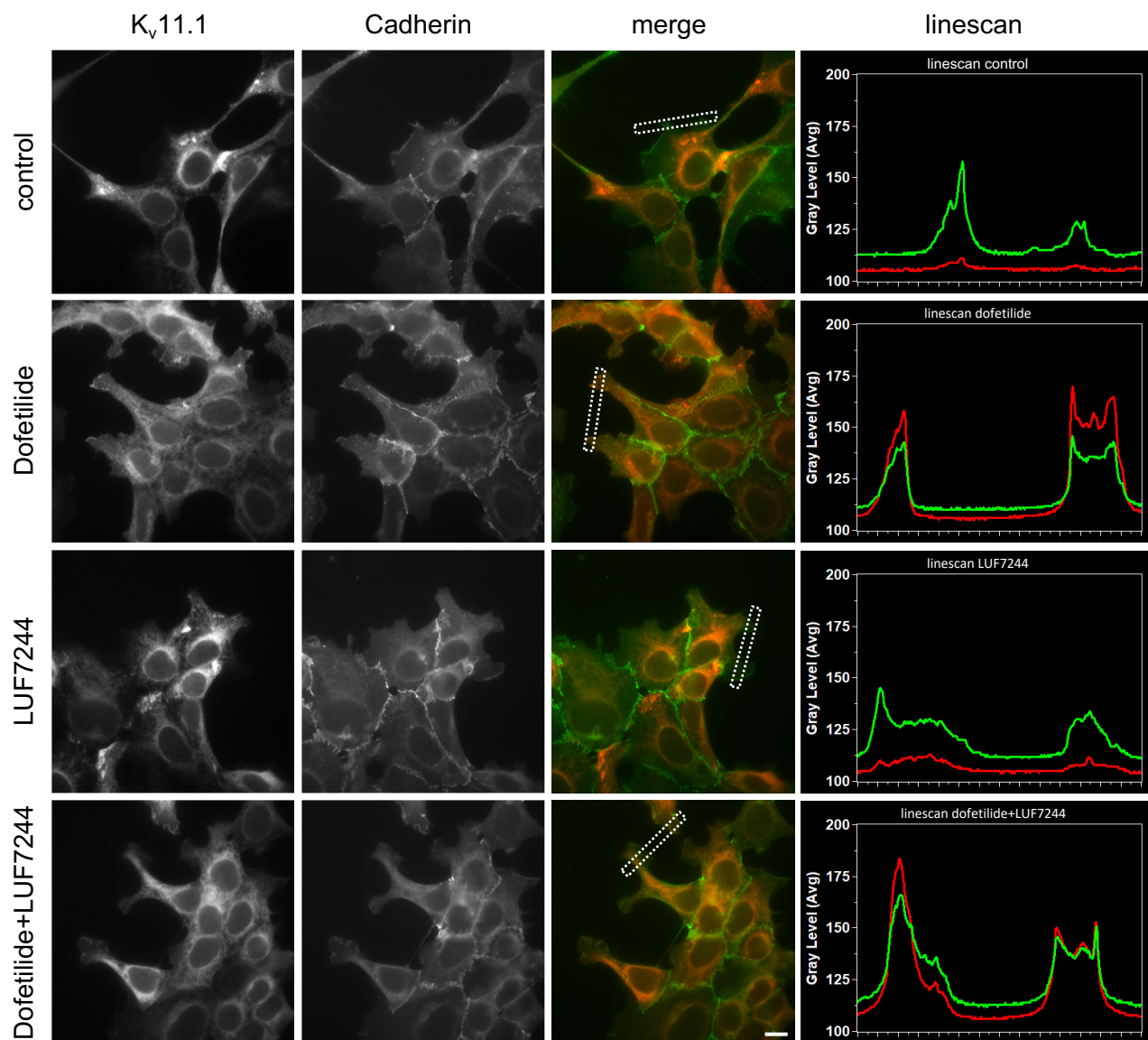


Figure 3



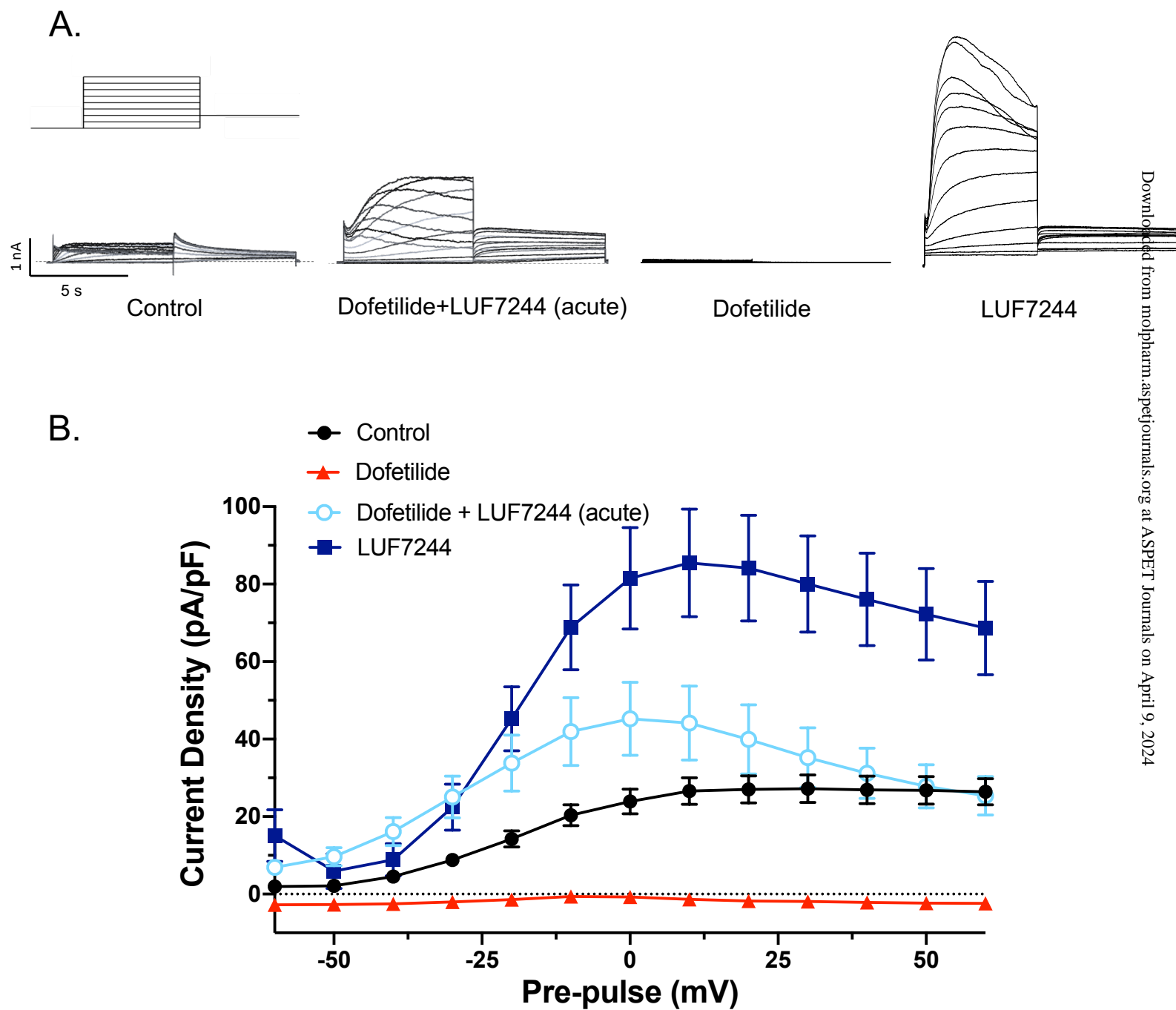


Figure 5

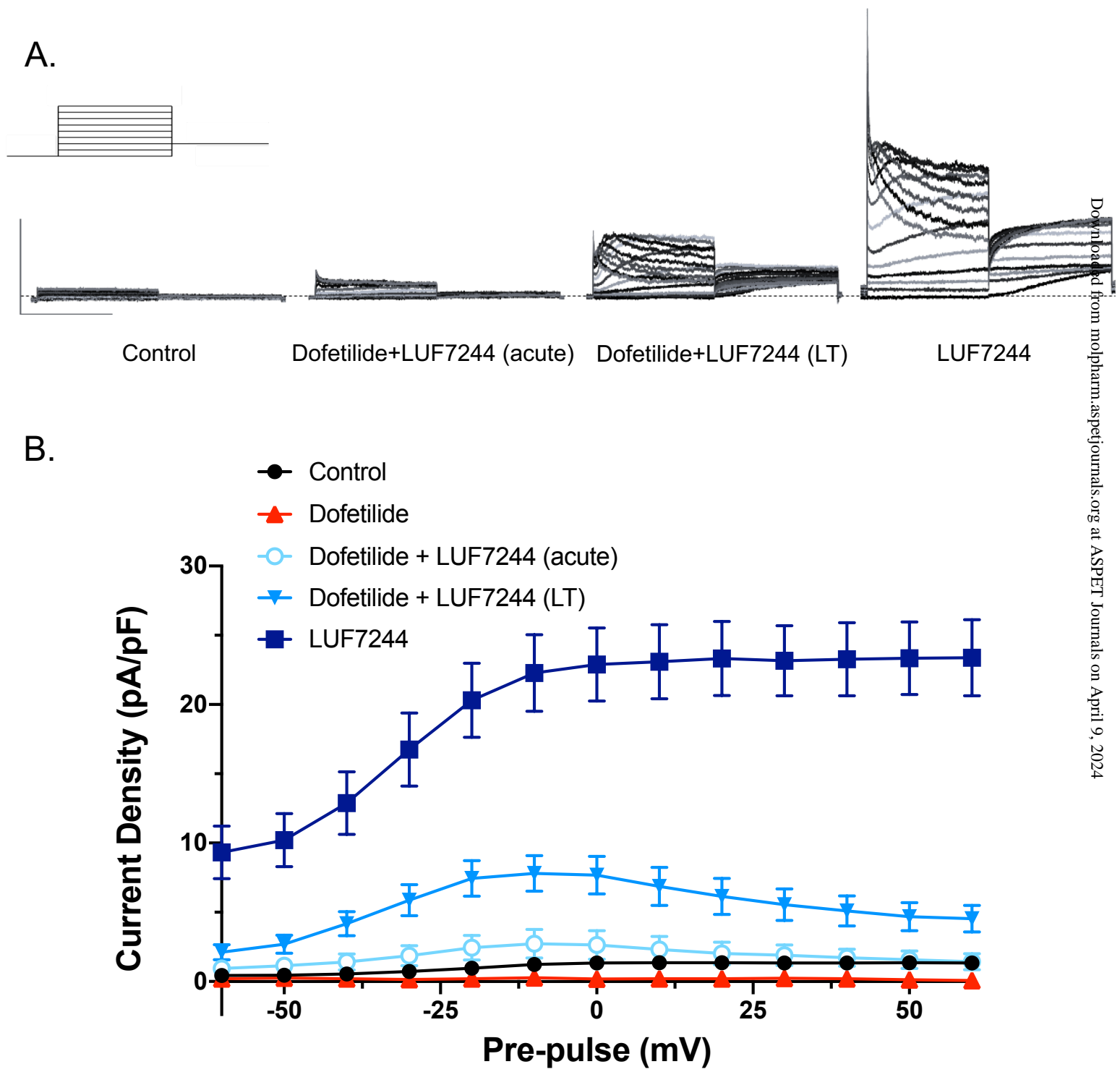


Figure 6